Vol. 679: 195–212, 2021
https://doi.org/10.3354/meps13894

MARINE ECOLOGY PROGRESS SERIES
Mar Ecol Prog Ser

Published November 25

Spatiotemporal models highlight influence of oceanographic conditions on common dolphin bycatch risk in the Bay of Biscay

Lola Gilbert[1,2,*], Etienne Rouby[1,2], Emilie Tew-Kaï[3], Jérôme Spitz[1,2], Hélène Peltier[1,4], Victor Quilfen[3], Matthieu Authier[1,4]

[1]Observatoire Pélagis, UMS 3462 Université de La Rochelle - CNRS, 17000 La Rochelle, France
[2]Centre d'Etudes Biologiques de Chizé-La Rochelle, UMR7372 Université de la Rochelle - CNRS, 17000 La Rochelle, France
[3]Shom, CS 92803-29228 Brest, France
[4]ADERA SAS, CS 60040-33608 Pessac Cedex, France

ABSTRACT: The population of short-beaked common dolphins *Delphinus delphis* of the Bay of Biscay (northeast Atlantic) has been subjected to potentially dangerous levels of bycatch since the 1990s. As the phenomenon intensifies, it represents a potent threat to the population. Here, we investigated the relationship between bycatch mortality and oceanographic processes. We assumed that oceanographic processes spatiotemporally structure the availability and aggregation of prey, creating areas prone to attract both common dolphins and fish targeted by fisheries. We used 2 datasets from 2012 to 2019: oceanographic data resulting from a circulation model and mortality data inferred from strandings. The latter allows location of mortality areas and quantification of the intensity of mortality events at sea. We fitted a series of spatiotemporal hierarchical Bayesian models using integrated nested Laplace approximations (INLA). Results provided first insights on how bycatch of common dolphins in the Bay of Biscay might be related to key seasonal and dynamic oceanographic features. We showed that from a statistical predictive point of view, the monthly trend of 2019 bycatch mortality could be predicted with few oceanographic covariates. This study highlights how gaining knowledge about environmental influences on interactions between short-beaked common dolphins and fisheries could have great conservation and management value. Identified relationships with oceanographic covariates were complex, as expected given the dynamic aspects of oceanographic processes, dolphins and fisheries distributions. Further research focusing on smaller time scales is needed to elucidate proximal drivers of common dolphin bycatch in the Bay of Biscay.

KEY WORDS: Spatiotemporal modelling · Reverse drift modelling · Prey–predator relationship · Sea surface temperature · Thermal fronts · Eddies

1. INTRODUCTION

Incidental catch, or bycatch (i.e. the undesired catch of nontargeted species in fishing gear), represents the most potent and well-identified threat to small cetaceans' populations (Reeves et al. 2005). Because they are long-lived species, cetaceans cannot sustain high rates of depletion (Lewison et al. 2004, Mannocci et al. 2012). Bycatch has already led populations or species to serious reduction (Reeves et al. 2005, Brownell et al. 2019) or even extinction (Turvey et al. 2007, Brownell et al. 2019), the vaquita porpoise *Phocoena sinus* Norris and MacFarland, 1958 (Norris & MacFarland 1958) being a potentially immi-

*Corresponding author: lola.gilbert@univ-lr.fr

nent example of the latter outcome (D'Agrosa et al. 2000, Jaramillo-Legorreta et al. 2007, 2019).

Short-beaked common dolphins *Delphinus delphis* Linné, 1758 in the Bay of Biscay (northeast Atlantic) have been subjected to potentially dangerous levels of bycatch since the 1990s (see Murphy et al. 2019 for a review). In France, the magnitude of bycatch is evidenced by high numbers of strandings of bycaught dolphin carcasses on the Atlantic seaboard. Mannocci et al. (2012) estimated that with 1000 bycaught individuals per year, the northeast Atlantic population could be reduced by 20% in 30 yr and could become extinct in a hundred. Still, the phenomenon has become more intense in the past decade. Since 2016, the number of strandings has increased every year (http://seamap.env.duke.edu). Bycatch estimates from strandings that occurred solely in the Bay of Biscay have been above what the population of common dolphins of the whole northeast Atlantic can theoretically sustain (Mannocci et al. 2012, Peltier et al. 2016, ICES 2020). From January to April 2019 alone, strandings suggested bycatch levels as high as 9500 individuals (95%CI: [6890; 14 200]) (Dars et al. 2019).

Stranding data can be complementary to data from European observer programs and can provide relevant information on cetacean bycatch (Peltier et al. 2016, IJsseldijk et al. 2020). In France, they have been instrumental to estimate the magnitude of common dolphin bycatch in the Bay of Biscay (Peltier et al. 2016) and to reveal a strong seasonality, with increased mortality in winter months (January to March) (Peltier et al. 2016, 2019, 2020, Dars et al. 2019). From 2016 onward, strandings of animals showing bycatch evidence have risen in summer (July and August), although to a lesser extent than in winter (Dars et al. 2019). Stranding data further made it possible to identify spatiotemporally varying mortality areas (as areas where carcasses of bycaught dolphins were released from fishing boats) through reverse drift modelling of carcasses trajectories (Peltier & Ridoux 2015, Peltier et al. 2016, 2021). In winter months, most bycatch events likely occur in the southern part of the continental shelf and slope (Peltier et al. 2016, 2020), resulting in strandings all along the shore from the south of the Finistère region to the border to Spain, whereas in summer most carcasses strand in southern Finistère (Fig. 1). Finally, the bycatch pattern displays high interannual variability, with different stranding levels and associated bycatch level estimates from year to year (Peltier et al. 2016).

Stranding data further revealed possible association between bycatch events and common dolphin preys. The reverse drift modelling of carcasses allowed the identification of some potentially high-risk fisheries and their caught fish species (Peltier et al. 2020, 2021). The analysis of stomach content of bycaught stranded animals suggested that most dolphins were feeding when death occurred. Moreover, some fish species targeted by common dolphins (e.g. mackerel or sardine) are also included in the diet of predatory fish species of fisheries interest (e.g. hake or seabass) (Spitz et al. 2013). Hence, changes in the local distribution and abundance of prey species might be a substantial driver of the co-occurrence of common dolphins, commercial fish species and fisheries in localized areas.

As marine mobile predators, cetaceans have a dynamic distribution integrating ecological processes across all levels of the trophic web (Croll et al. 1998, Barlow et al. 2020). The proximal relationship between prey and predator could drive the spatiotemporal variability of the bycatch pattern: fish distribution is notoriously variable in both space and time (Hyrenbach et al. 2000) and is governed by many factors ranging from dynamic oceanographic conditions to each species' annual cycle. In this study, we aimed at assessing the influence of oceanographic

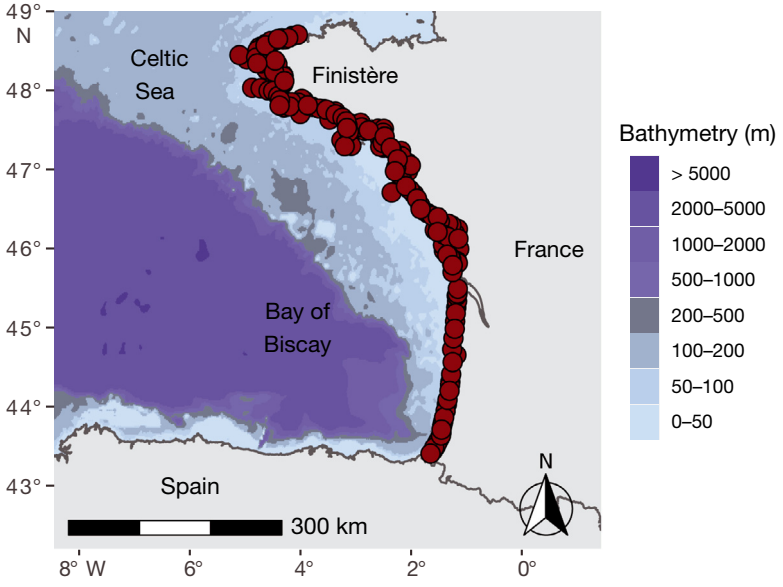

Fig. 1. Study area showing bathymetry and geographic references mentioned in the text, and location of common dolphin stranded carcasses used for the study (red dots)

processes on bycatch of common dolphins in fishing gear. We thus focused on the distal relationship between marine predators and oceanographic processes. We assumed oceanographic processes spatiotemporally structure the availability and aggregation of prey, creating areas prone to attract common dolphins and predatory fish targeted by fisheries and consequently increase the bycatch risk. For instance, meso and submesoscale processes such as fronts (where 2 joined water masses differ by their density), upwelling or eddies enhance the enrichment, concentration and retention of nutrients (Bakun 1996). These processes facilitate the development of trophic networks, from phytoplankton to zooplankton, to fish and finally, to apex predators (Bakun 1996, 2006).

Knowledge of oceanographic conditions is readily available from either remote sensing or modelling. This information is therefore commonly used to make inferences about prey availability and species distribution (Forney 2000, Becker et al. 2010, Best et al. 2012, Stephenson et al. 2020). Oceanographic data have been previously used in the context of bycatch studies, either to identify high risk areas through the association of species distribution modelling and distribution of fishing effort (Žydelis et al. 2011, Murray & Orphanides 2013, Di Tullio et al. 2015, Díaz López et al. 2019) or to identify possible drivers of bycatch events (Gardner et al. 2008, Cosandey-Godin et al. 2015, Hahlbeck et al. 2017, Scales et al. 2018). Cosandey-Godin et al. (2015) suggested the forecasting of high bycatch risk areas to identify mitigation measures. We investigated relations between mortality of common dolphins in fishing gear and oceanographic processes in the Bay of Biscay. Predicting high bycatch areas was beyond the scope of this paper, although it constitutes a promising venue for further investigations.

This work capitalized on 2 sources of data: the bycatch–mortality index inferred from strandings and fine-scaled essential oceanographic variables (EOVs) (García-Barón et al. 2020, Tew-Kai et al. 2020). We selected physical variables significantly contributing to the characterization of the ocean realm (Tew-Kai et al. 2020). We used hierarchical Bayesian models to account for spatiotemporal processes: bycatch mortality areas, oceanographic processes, and common dolphin and fisherie distributions are dynamic in both space and time. The area of study was limited to waters of the Bay of Biscay, with a small part of the Celtic Sea (Fig. 1). After model fitting, we used out-of-sample, 1-step-ahead prediction to predict bycatch mortality in 2019 from oceanographic processes.

2. MATERIALS AND METHODS

2.1. Dolphin mortality index from stranding data

2.1.1. Mortality index

For most bycatch events, no data or location at sea is available. However, some bycatch events are detectable from the stranding of common dolphins presenting bycatch evidence (Kuiken 1994). To determine the origin of carcasses, a reverse drift trajectory can be computed with the drift prediction model MOTHY (Modèle Océanique de Transport d'Hydrocarbure, developed by Météo France; Daniel et al. 2002), integrating drift conditions and characteristics of dolphins' carcasses (see Peltier & Ridoux 2015, Peltier et al. 2012). Reverse drift trajectories of bycaught animals were used to compute a mortality index (MI) to identify probable mortality areas and to quantify the intensity of mortality events at sea in space and time (Fig. 2).

From 2012 to 2019 stranding data, only carcasses presenting bycatch evidence or which stranded during an intense mortality event were selected. Intense mortality events are when more than 30 dolphins strand on 200 km of coastline within 10 d (Peltier et al. 2016). We further selected carcasses with estimated mortality windows up to 15 d (2384 out of 4544, i.e. 52%). For each carcass, a reverse drift trajectory was calculated with MOTHY, with one point every 10 h. Drift tracks were limited from 0 to 5 or from

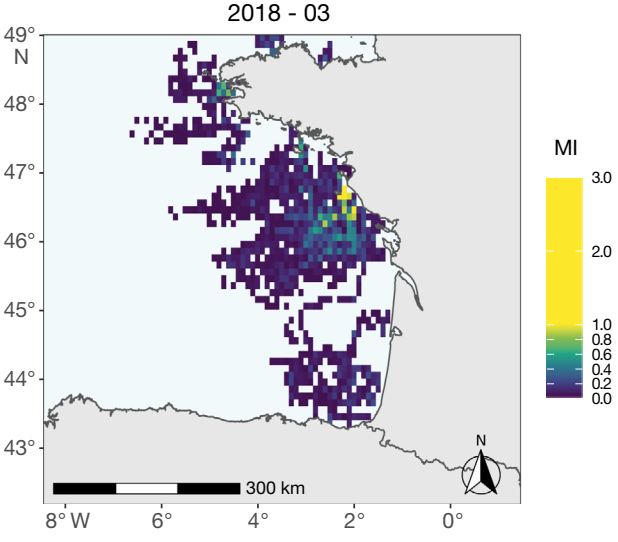

Fig. 2. Spatialized mortality index (MI) for March 2018. MI was computed from reverse drift modelling of stranded carcasses of common dolphins showing bycatch evidence. It allows us to locate potential mortality areas and to quantify the intensity of mortality events

5 to 15 d depending on the mortality window estimated from the decomposition state of the stranded carcasses. The computation of the MI on a daily basis, using a regular grid of 0.1° × 0.1° resolution (i.e. approximately 26 nmiles^2 or 89 km^2) for the Bay of Biscay, assumed an equal probability of bycatch occurring at each drift point. For a day d, a grid cell c and a carcass i, MI was defined as follows:

$$\mathrm{MI}_{d,c,i} = \frac{\text{No. of drift points of } i \text{ in grid cell } c}{\text{Total no. of drift points of } i} \quad (1)$$

The more a carcass stagnates in a grid cell, the higher MI reflects a higher probability that death occurred in that grid cell. For a given cell on a given day, there could be reverse drift points associated with several carcasses. The total MI for d and c was then:

$$\mathrm{MI}_{d,c} = \sum_{i} \mathrm{MI}_{d,c,i} \quad (2)$$

The greater the number of carcasses that have drifted through a grid cell, the higher its MI. Finally, daily MIs were summed for each grid cell over each month from 2012 to 2019 resulting in the following spatial monthly MI, for month m and grid cell c (Fig. 2):

$$\mathrm{MI}_{c,m} = \sum_{d \in m} \mathrm{MI}_{d,c} = \sum_{d \in m} \sum_{i} \mathrm{MI}_{d,c,i} \quad (3)$$

The total sum of MI over each month is equal to the number of stranded dolphins included in the dataset. In total, 1789 carcasses stranded all along the shore of the Bay of Biscay (Fig. 1) were used for the present study, with substantial seasonal and inter-annual variations (Fig. 3). Monthly numbers are provided in Supplement 1; www.int-res.com/articles/suppl/m679p195_supp/.

2.1.2. Stranding probability

A wide range of factors lead a carcass to strand, including buoyancy (the carcass must be floating) and drift conditions (wind being one of the main drivers). Consequently, not all carcasses of bycaught common dolphins do strand (Peltier et al. 2016). Drift conditions can sometimes keep carcasses at sea rather than push them to the coast. Buoyancy of carcasses is probably influenced by several parameters (i.e. depth at which death occurred, buoyancy at time of death; Moore et al. 2020) so that they may either sink or float when they are released from fishing boats. The calculated MI thus contained 'false' zeros, associated to grid cells where conditions would not have led to strandings if carcasses happened to drift through them. Conversely, 'true' zeros were associated to grid cells where conditions could have led drifting carcasses to strand. To account for this, we systematically included stranding probability as a covariate in all models. Stranding probabilities were estimated from drifts of simulated dolphin carcasses with MOTHY (Peltier et al. 2013, 2014, 2016). It was calculated over 10 d periods and averaged over each month. A conditional autoregressive (CAR) model was then applied to the result to leverage spatial dependence and smooth estimated probabilities. The spatial resolution of estimated probabilities was larger than that of MI (Fig. 4): each grid cell of the MI grid was matched to its closer neighbour in the stranding probability grid (using R package sf of Pebesma 2018). True zeros should be associated with high stranding probabilities whereas false zeros should be associated with low stranding probabilities.

2.2. Oceanographic data

Monthly EOVs and derived variables were computed from the 3-dimensional HYCOM numerical model of the French Service Hydrographique et Océanographique de la Marine (Shom). Based on the original HYCOM model (Bleck 2002), it was set with a number of numerical developments to optimize the model for coastal zones (Pichon & Correard 2006, Morel et al. 2008, Lahaye et al. 2011) and has already been successfully used over the Bay of Biscay area (e.g. Pichon et al. 2013). Hindcasts were calculated hourly from 1 January 2012 to 31 December 2019 to compute monthly EOVs and derived variables. EOVs are outputs of the model (temperature, salinity, cur-

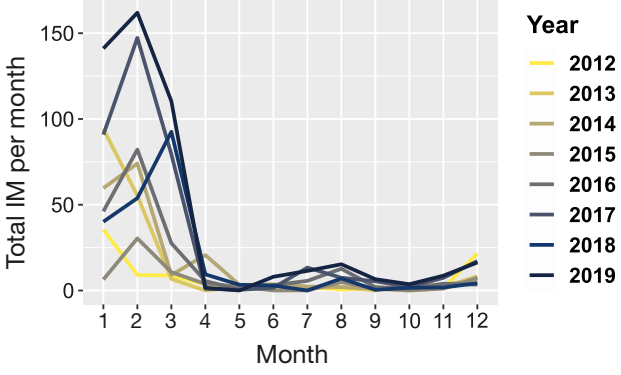

Fig. 3. Evolution of the total mortality index (MI) per month and per year. The monthly sum of spatial MI over the study area is equal to the number of stranded dolphin carcasses for which a reverse drift was calculated, thus giving a mortality signal

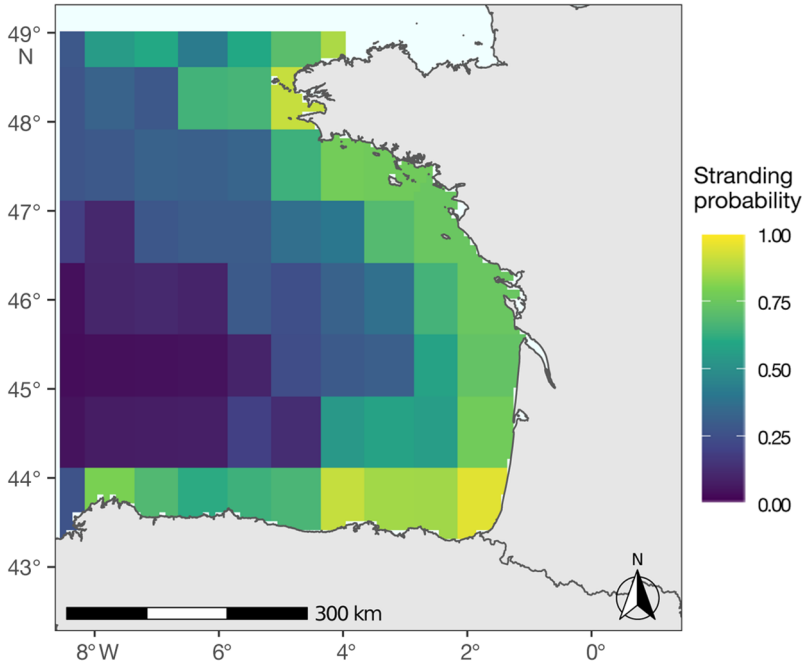

Fig. 4. Stranding probability in March 2018, estimated from simulated drifts of common dolphins, then smoothed with conditional autoregressive (CAR) model to account for spatial dependency between adjacent cells

rent), and derived variables have been calculated from these EOVs. One EOV and 2 derived variables, hereafter referred as oceanographic variables (OVs), were integrated in this study: (1) the sea surface temperature (*sst*), (2) the mean sea surface temperature gradient (*mean_sst_grad*), quantifying the intensity and wideness of thermal fronts, and (3) eddy kinetic energy (*eke*), quantifying the turbulent component of the residual (non-tidal) surface current. *sst* was chosen for its strong seasonal component (Lambert et al. 2017) but also as it is commonly integrated in habitat modelling of multiple marine taxa (Doniol-Valcroze et al. 2007, Mellin et al. 2012, Hughes et al. 2014, Castro et al. 2020). In addition, thermal fronts and eddies have been identified as key structures for the conservation of marine predators (Scales et al. 2014, 2018). Such interfaces might trigger bottom-up processes. As nutrient mixing and retention in the photic zone can boost primary productivity, interfaces like fronts and eddies might attract apex predators through a cascading effect from the lower trophic levels to the highest ones (Bakun 1996, 2006, Scales et al. 2014). This association was observed for several marine predators (Nel et al. 2001, Doniol-Valcroze et al. 2007, Bailey & Thompson, 2010, Miller et al. 2015, Snyder et al. 2017) along with further associations with bycatch events (Hahlbeck et al. 2017, Scales et al. 2018). Moreover, the Bay of Biscay encompasses a shelf area with complex dynamic mesoscale processes following a seasonal cycle (Yelekçi et al. 2017), and we meant to integrate some of these features in our analysis through the dynamic variables *eke* and *mean_sst_grad*.

As the spatial resolution of the oceanographic data was the nautical mile, it was upscaled to match that of the MI. All data can be visualized through maps and histograms at http://pelabox.univ-lr.fr:3838/pelagis/DdSeaByc/ (Tab: '1. Data').

2.3. Spatiotemporal modelling framework

Our goal was to elucidate if oceanographic conditions were associated with bycatch of common dolphins in fishing gear with statistical modelling. We considered a general set up MI ~ OVs where MI is the response variable whose variations are to be correlated with OVs, with linear effects for covariates.

2.3.1. Spatial and temporal considerations

Common dolphin bycatch — and stranding of animals showing bycatch evidence — is a seasonal phenomenon in the Bay of Biscay (Dars et al. 2019, ICES 2020). The mortality signal, defined here as the number of stranded common dolphin showing bycatch evidence, is higher in January to March (winter) and in July and August (summer) but is lower in between (Fig. 3). Oceanographic conditions also follow a seasonal cycle with different dynamics in winter and summer and transition regimes in between (Yelekçi 2017). Our exploratory analysis (not shown here) suggested that the relationship between the response variable and oceanographic covariates varies across months. Hence, we chose to fit one model per month to get a climatology over the study period. Each monthly model gathered data for the corresponding month from 2012 to 2019, resulting in 12 models (from January to December). A similar approach was used in Foravanti et al. (2021). This climatological approach had the advantage of reducing computational cost.

The relation between OVs and MI in one given month can vary from one year to the next, for in-

stance because of a timelag in cyclic phenomena (Huret et al. 2018) or because of singular climatic events. The dynamic of mesoscale processes is complex in the Bay of Biscay (Yelekçi 2017). Singular phenomena could be especially attractive for preys of dolphins and predatory fish targeted by fisheries depending on their extent, their duration and their time of occurrence. The effect of OVs on bycatch risk (and thus on MI) must be varying in time, as suggested by the intensification in strandings from 2016 (Dars et al. 2019). This led us to consider annually varying coefficients for OVs (i.e. random slopes). We further added an annually varying intercept (random intercept) to account for different annual levels of bycatch. Using random slopes amounts to considering an interaction with year: time-series of the effect of OVs on MI for each month and each year were an output from models over the study period.

Generalized linear models (GLM) and generalized additive models (GAM) usually assume all relevant covariates have been included in the model (Zuur et al. 2007a,b). This assumption is unrealistic in most cases, and omitted variables may result in a residual dependence that, if not accounted for, may result in misleading inferences (Legendre et al. 2002, Valcu & Kempenaers 2010). Omitted variables bias may manifest in residual autocorrelation, either temporal, spatial, or both. Because there was one model per month, the time lag between each 'measurement' was 11 mo, and we assumed no temporal autocorrelation. Yet, spatial autocorrelation, if not taken into account, could suggest spurious correlations with OVs. Consequently, all models included explicitly a spatial component in addition to the (implicitly spatial) OVs.

2.3.2. Hierarchical Bayesian framework and Gaussian random field

We used a hierarchical Bayesian framework as they are adapted to the modelling of complex spatial or spatiotemporal phenomena (Cosandey-Godin et al. 2015, Martínez-Minaya et al. 2018). Including a spatial random effect, e.g. with a Gaussian random field (GRF), is straightforward (Blangiardo et al. 2013, Cosandey-Godin et al. 2015). The GRF, indexed on each grid cell, is a stochastic process that will gather all the spatially implicit information in the data that are not accounted for by other model components, in our case oceanographic covariates (Cosandey-Godin et al. 2015). To model this random field, we chose a CAR process (Besag et al. 1991, Besag & Kooperberg 1995) based on the notion of nearest neighbours (the so-called first law of geography: 'Everything is related to everything else, but near things are more related than distant things'; Tobler 1970, p. 236). For the vector of grid cells ($\eta_1, \eta_2, \ldots, \eta_n$, here n = 3487) it can be written as follows:

$$\eta_i \,|\, \eta_j,\ i \neq j,\ \tau \sim N\left(\frac{1}{n_i},\ \frac{1}{n_i \times \tau}\right) \tag{4}$$

where n_i is the number of neighbours for grid cell i and τ is a precision parameter. $i \sim j$ means that the 2 grid cells i and j are neighbours.

2.3.3. Model set up

MI was first transformed to log(MI + 1) and then modelled by a Gaussian distribution with an identity link function. The spatial CAR process was considered constant over years, so that there would be one spatial field per month. The stranding probability (SP) was always included as a covariate with a linear effect. For oceanographic variables effects and for the intercept, we included the possibility for the coefficients to vary from one year to the next by specifying a Gaussian random (independent and identically distributed) effect on years (random slopes). For an overview of our monthly model, we had for the response variable MI in year t and grid cell c, with oceanographic covariates X:

$$\begin{cases} \text{For all } m \text{ in } 1{:}12 \text{ (dropping the } {}_m \text{ subscript below for clarity)} \\ \log(\mathrm{MI}_{c,t}+1) \sim N(\pi_{c,t},\ \sigma) \\ \mathrm{Id}(\pi_{c,t}) = \gamma \times \mathrm{SP}_{c,t} + \beta_{0,t} + \sum_j \beta_{j,t} \times X_{j,c,t} + \eta_c + \varepsilon_{c,t} \end{cases} \tag{5}$$

where N defines the normal distribution of location parameter $\pi_{c,t}$ and scale parameter σ, Id is the identity link function, γ the coefficient associated with SP, $\beta_{0,t}$ the intercept for year t, $\beta_{j,t}$ the annual coefficient of covariate $X_{j,c,t}$ at cell c in year t and η_c the spatial effect associated to grid cell c, which is assumed to result from a CAR model. Finally, $\pi_{c,t}$ are unstructured errors, i.e. residuals. Parameters estimated in the linear predictor, i.e. γ, $\beta_{0,t}$, $\beta_{j,t}$, η_c and $\pi_{c,t}$ constitute the latent field. They are assumed to follow Gaussian distributions (Rue et al. 2009). These parameters depend on a vector of hyperparameters θ that are not necessarily Gaussian (Rue et al. 2009). In this manner, the monthly model defined in (Eq. 5) is a latent Gaussian model (LGM) (Rue et al. 2009). It presents a spatial component (η_c) along with annual components ($\beta_{0,t}$ and $\beta_{j,t}$).

2.3.4. Inference with integrated nested Laplace approximations (INLA)

Inference for such complex spatial models is computationally demanding and requires approximation to be fully scalable with a large amount of data. For a large dataset with 3487 grid cells observed 8 times (i.e. years) per analysis, i.e. 27 896 observations per month, classical methods like Markov Chain Monte Carlo may be prohibitively slow (Blangiardo et al. 2013). We used INLA, which offers a very efficient alternative giving fast and reasonable estimations (Rue et al. 2009). Especially adapted to LGMs, this algorithm uses a combination of analytical approximations and numerical integration for the inference of posterior marginals and likelihood, which greatly reduce computational demand while being extremely accurate (Rue et al. 2009, Moraga 2019). Inference with INLA was carried out with the R-INLA package in R statistical software v4.0.2 (R Core Team 2020).

Before model fitting, all oceanographic variables were standardized (mean-centered and scaled to unity), and *eke* and *mean_sst_grad* were log-transformed to account for skewness and strict positivity. Weakly informative priors were chosen so that estimations would mostly be driven by the data (Gabry et al. 2019). Fitted and predicted values that were negative after back transformation were set to zero.

2.3.5. Model selection

All possible combinations of the different effects and covariates were tested, with the SP systematically included as a confounding factor (list of tested models is provided in Supplement 2). The first combinations were the simplest models with only linear effects for oceanographic covariates (i.e. in Eq. 5, β_j replaces $\beta_{j,t}$) and no spatial field (8 possibilities with the null model). Second, coefficients were allowed to vary between years for oceanographic covariates (7 possibilities) with random slopes. Finally, the CAR process was added, with and without oceanographic covariates, considering strict linear effects or annual random slopes (15 possibilities). The 30th model was the more complex, defined in Eq. (5), where $j \in [1,3]$ and X_j are thus *sst*, *eke* or *mean_sst_grad*. Model selection was conducted using the Wanatabe Akaike information criterion (WAIC) (Watanabe 2010). WAIC gives an approximation of the out-of-sample predictive accuracy using the in-sample data (Gelman et al. 2014).

2.3.6. Model checking

The coefficient of determination R^2 for each monthly model was computed. R^2 is the proportion of variance in the response variable accounted for by explanatory variables (Johnson 2014). We apportioned the total variance to different model components, i.e. spatial or annual, and assessed their respective contributions. For random slopes models, some variance components depend on observations (Johnson 2014). For instance, the variance of $\beta_{sst,t}$, coefficient of variable *sst* on year *t*, depends on values of *sst* during year *t*. We used the matrix formula (11) of Johnson (2014); see Supplement 3 for further details.

Finally, we assessed the predictive power of models, first by conducting out-of-sample cross-validation (CV), then by testing different prediction scenarios. While the dataset was complete from 2012 to 2018, for 2019 only values of oceanographic variables were given to get predictions of MI for this year. As the intercept and covariates coefficients were estimated annually, there was an index associated to each year. For the CV procedure, we considered 2019 as a new year (predicted from the posterior distribution) and attributed to this year a new and unique index. In addition, we tested different repetition scenarios (RS): instead of attributing a new index to year 2019 and consider it as a new sample, we considered 2019 as a repetition of a previous year by attributing to 2019 its index. This way, all model components fitted during the 'repeated' year were used (covariates' coefficients, effect of the stranding probability, spatial CAR process) for the prediction of MI in 2019, still considering 2019's oceanographic conditions. We tested all 7 possibilities, i.e. we considered 2019 as a repetition of 2012, then of 2013, 2014, 2015, 2016, 2017 and 2018. Then, we confronted the predicted total mortality for 2019 to 2019's total mortality from the dataset (never seen by the models). We also computed a root mean squared error (RMSE) per RS and for the CV, based on the monthly differences between predicted and observed (from strandings) total monthly mortality. With these repetition scenarios, we aimed at addressing whether oceanographic conditions of past years affected bycatch mortality risk in the same way and could predict the observed mortality in 2019.

3. RESULTS

3.1. Model selection

For most months, the most complex model detailed in formula (Eq. 5) had the smallest WAIC values (table with WAIC of all tested models provided in Supplement 4). It included a CAR process, year-varying intercepts and year-varying slopes for the 3 covariates *sst*, *eke* and *mean_sst_grad*. In May, June and November the model with the smallest WAIC values excluded *eke* and for September *sst* was excluded. However, the difference in WAIC between these models and the most complex one selected for other months was small (relative difference of 0.01, 0.03, 0.1, 0.06% in May, June, September and November, respectively). Hence, we chose to keep the most complex model with all 3 covariates for all months to facilitate comparison of results over the 12 months.

3.2. Oceanographic covariates effects on the MI

Slope estimates of the effect of *sst*, *eke* and *mean_sst_grad* on spatiotemporal MIs were precise with tight credible intervals (see http://pelabox.univ-lr.fr:3838/pelagis/DdSeaByc/; Tab: '2. Results 2.1.'. There were no estimates for year 2019 as this year was not used in model fitting but in out-of-sample, 1-step-ahead cross-validation and predictions. Overall, effects were more intense in the winter season, from January to March (Fig. 5). They were close to zero for the rest of the year, except in July and August for 2016, 2017 and 2018 for *eke* and *mean_sst_grad*. The winter variation pattern of the effect of *eke* and *mean_sst_grad* was different every year. Their effect on MI was sometimes positive and sometimes negative, depending on years. In July and August, however, the effect of these 2 covariates was consistent from 2016 to 2018. It was negative for *eke* and positive for *mean_sst_grad*. The winter variation pattern of the effect of *sst* was consistent between years, with interannual differences in its intensity. It switched sign from one month to the next, for most years. In summer, the effect of *sst* was close to zero, except in 2017, when it was slightly negative. For all 3 covariates, 2017 emerged as a singular year.

The intercept was estimated as a mean level of MI with OVs being set at their mean values (given that they were standardized, that is mean-centered). It was greater in winter, with mostly positive values in January and February but negative values in March, except in 2017, when it was positive for all 3 months (Fig. 5). Its pattern of variation was more or less consistent over the study period, with differences in its intensity. In summer, the intercept was slightly positive only in 2016 and 2017.

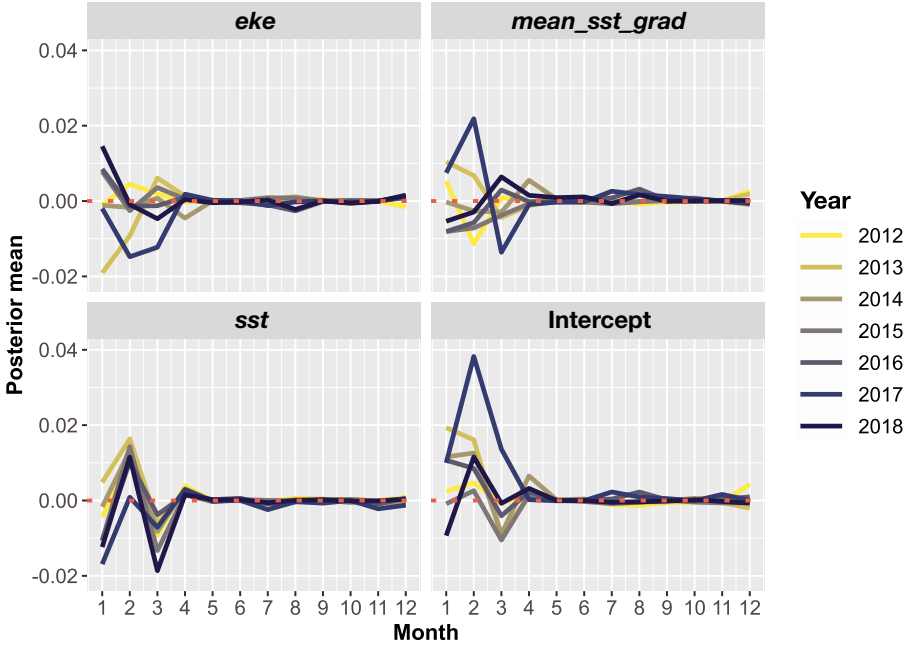

Fig. 5. Means estimates from the 12 separated monthly models of intercepts and coefficients of oceanographic covariates, for each month and each year. Spatiotemporal monthly models were inferred with integrated nested Laplace approximations (INLA). *eke*: eddy kinetic energy; *mean_sst_grad*: mean sea surface temperature; *sst*: sea surface temperature

3.3. Variance partitioning

The computation of R^2 allowed us to differentiate the contribution of the different model components to integrate MI variations (Fig. 6). The annual component included annual coefficients of covariates (random slopes) along with annual intercepts. The spatial component was the CAR process whose contribution in variance showed little between-month variation. The residual component included what was not accounted for by either of the 2 precedent components. In total, models better accounted for MI variations from January to April, the annual component being the most contributive component on this period. From January to March, 21 to 25% of the variance were accounted for by annual and spatial components. A rise in the annual component contribution in July and in the spatial component contribution in August resulted in a rise in the overall variance accounted for these 2 months. Afterward, most of the variations of MI were integrated in residuals. Note that, using formula (11) of Johnson (2014), covariances between components were included: some negative covariances terms explain that contributions of the 3 components naïvely sum to more than 100% for some months.

3.4. CV and predictions of 2019 mortality with repetition scenarios

For CV, 1-step-ahead prediction was performed. Each monthly model was calibrated on 2012–2018 data, so MI data from 2019 was not used in model fitting. 2019 oceanographic data were thus used for prediction, taking between-year variations into account. The total monthly MI of the dataset (observed) for 2019 fell within the confidence interval of total monthly predicted values, for both the winter and the summer mortality periods (Fig. 7). Total mean predicted values were below observed ones. In addition, 2019 was assumed as a repetition of each year between 2012 and 2018 (RS), to highlight if past oceanographic influences could predict observed mortality in 2019. Among the 7 RS, observed values of total monthly mortality of 2019 during the winter mortality period was within (or close to) confidence intervals of predicted values for 2 RS, when 2019 was considered as a repetition of 2013 (RS 2019 = 2013) and as a repetition of 2017 (RS 2019 = 2017) (Fig. 7). For RS of other years, predicted values and confidence intervals were lower than observed monthly mortality, from January to March. The summer mortality season was not reproduced by the models for RS of years before 2016. Overall, 2017 RS showed the lowest RMSE and gave the best prediction of 2019 monthly mortality levels (Table 1). RMSE for CV was below RMSE of RS of years 2012 and 2015 and close to that of 2018.

Additional results such as maps of fitted or predicted values and maps of the estimated spatial effects are available at http://pelabox.univ-lr.fr:3838/pelagis/DdSeaByc/ (Tab: '2. Results') for all 12 months. A temporal series of total monthly mortality of fitted values and observed values are provided in Fig. A1 in the Appendix.

4. DISCUSSION

We assumed bycatch risk could be correlated to the proximal relationship between the dynamic distribution of common dolphins, commercial predatory fish species targeted by fisheries and that of their common prey species, the latter being partially driven by oceanographic processes. Spatiotemporal information on at-sea bycatch mortality, fisheries, dolphins and fish prey species distribution is not easily accessible to study this proximal relationship. Thus, we used proxies, a mortality index inferred from strandings and oceanographic descriptors, to study the dis-

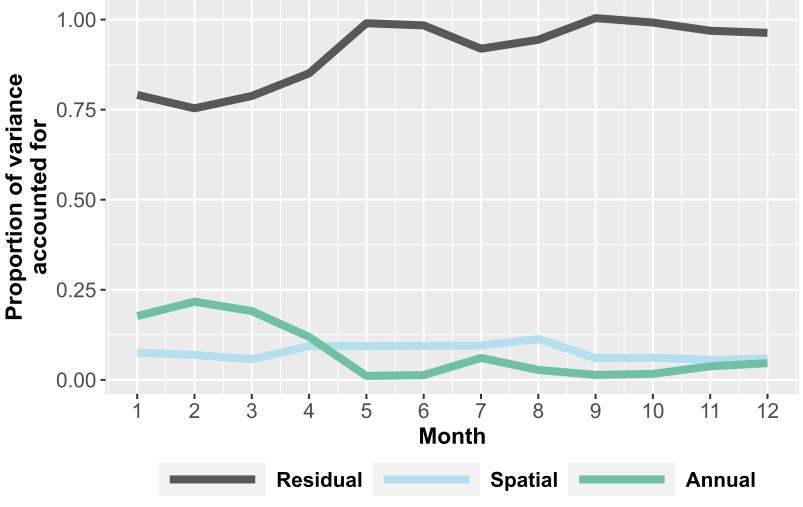

Fig. 6. For each of the 12 spatiotemporal monthly models inferred with integrated nested Laplace approximations (INLA), proportion (transformed with a square root) of variance accounted for by each model component. Residual: residual component; Spatial: spatial component (defined by a Gaussian random field); Annual: annual intercepts and coefficients of covariates

tal relationship between common dolphin bycatch and oceanographic processes. We mobilized 8 yr of stranding data (from 2012 to 2019) and explored spatial and temporal links between basal and apex nodes of the trophic network, from oceanographic processes to short-beaked common dolphins (and fisheries). We fitted a series of 12 spatiotemporal monthly models that included 3 oceanographic variables as covariates potentially contributing to the spatiotemporal structuring of bycatch risk of common dolphins in the Bay of Biscay. Results provided first insights into how the intensity of common dolphin bycatch in the Bay of Biscay might be modulated by key seasonal and dynamic oceanographic features.

4.1. Two seasons of mortality, two different underlying processes

Strandings highlight 2 seasons of high bycatch mortality in the Bay of Biscay: a main one from January to March and another (only observed from 2016 onward) in July and August (Fig. 3). Results reflected different patterns for these 2 mortality seasons, suggesting differences between the underlying phenomena leading to bycatch mortality. Outside these seasons, the explanatory power of oceanographic processes was very limited, and the effect of OVs on the mortality index was close to zero. Thus, it seems that OVs seasonally affect bycatch risk and should not be considered as season-invariant drivers of bycatch mortality.

4.1.1. Winter high mortality season, from January to March

The annual component, including OVs, accounted for most variations in bycatch risk during the winter mortality season (Fig. 6), suggesting a substantial influence of the oceanographic processes. Moreover, January, February and March were the months when OVs had the strongest effects on bycatch risk (Fig. 5). Depending on OVs, their effects (i.e. monthly estimated linear coefficients) showed different inter-annual patterns. The month-to-month effect of sea surface temperature was the only one to be consistent from one year to the next. Sea surface temperature partially drives the distribution and seasonal migrations of multiple marine taxa, from small pelagic fish (Lanz et al. 2009, Hughes et al. 2014,) to bigger fish (Hahlbeck et al. 2017) and high-level predators (Weltz et al. 2013). In the Bay of Biscay, the influence of sea surface temperature affects the distribution of identified prey species of common dolphins and commercial predatory fish species (Spitz et al. 2013), such as anchovies and sardines (Planque et al. 2007, Petitgas et al. 2014, Politikos et al. 2015). Therefore, a correlation between mortality and sea surface temperature can be expected if the underlying mechanisms are linked to preys of both common dolphins and commercial fish species targeted by fisheries. The effects of the mean temperature gradient and eddy kinetic energy were of the same magnitude as that of sea surface temperature but presented high inter-annual variations. Mean temperature gradient quantifies the intensity and wideness of thermal fronts, whereas eddy kinetic energy is associated with turbulent surface features such as eddies. Because they were averaged over each month, they should refer to relatively persistent structures. In winter, the Bay of Biscay environment is characterized by a seasonal cross-shore (west to east) surface temperature gradient with lowest temperature close to shore and intense frontal activity parallel to the coast (north to south) (Yelekçi et al. 2017). These frontal structures are freshwater fronts, correlated with the mixing of oceanic waters and cold freshwater inputs from river plumes (Yelekçi et al. 2017). Their location and timeline concur with observed patterns regarding bycatch mortality: during winter months, strandings were from all the Atlantic coast (http://seamap.env.duke.edu), and high mortality areas were previously identified on the continental shelf (Peltier et al. 2021). Moreover, most of highest MI values were located offshore of the coast from the south of the Finistère region to the south French border (not shown, see http://pelabox.univ-lr.fr:3838/pelagis/DdSeaByc/; Tab: '1. Data'), especially in 2017 when strandings were the more numerous over the 2012 to 2018 period. Together with the effects of the associated OVs on the MI, results suggested these seasonal fronts may be targeted by both fisheries and common dolphins as areas where fish aggregate, thereby putting the latter at risk of bycatch by the former.

4.1.2. Summer high mortality season in July and August

July and August were the only 2 other months when OVs accounted for a non-negligable fraction of variations in bycatch mortality (Fig. 6). The amount of total explained variance accounted for by OVs (included in the annual component) was more limited compared to the winter mortality season and was below the contribution of the CAR process. This could suggest that, during this summer season, other drivers (currently

omitted in the model) might drive mortality risk. However, this was expected as strandings are at least one order of magnitude lower in summer and only became substantial from 2016 onward. Nevertheless, different patterns emerged regarding the effects of oceanographic covariates. Conversely to the winter season, the sea surface temperature coefficient was close to zero for all years, and the effects of mean temperature gradient and eddy kinetic energy on the MI were, respectively, quite consistent for all 3 years when a summer mortality peak was observed (2016, 2017, 2018). For these 3 years and in July and August, the effect of the mean temperature gradient was slightly positive, meaning that thermal fronts were associated with higher MI and that of eddy kinetic energy was slightly negative, meaning that bycatch mortality probably occurred in low turbulence waters. In July and August, the mesoscale dynamic activity of the Bay of Biscay is rather different than in winter. In winter, the frontal activity in the Bay of Biscay is dominated by freshwater fronts resulting from input of cold freshwater from rivers whereas in summer, there are mainly fronts due to tidal flow (Yelekçi 2017). Winter freshwater fronts display more spatiotemporal variability (on a given year and interannually) as they are directly correlated to river flows (Yelekçi et al. 2017). Summer tidal fronts are conversely quite consistent from one year to the next because they are correlated to a repetitive process (i.e. tides) (Yelekçi et al. 2017). During summer, the main frontal activity is a seasonal tidal front, called the Ushant Front, and it is located in front of the French Finistère region (Yelekçi et al. 2017). Its activity peaks in July and August (Yelekçi et al. 2017). Turbulent components of surface currents are relatively low around this structure (not shown, see http://pelabox.univ-lr.fr:3838/pelagis/DdSeaByc/; Tab: '1. Data'), except at its most northern part. Again, the location of this typical frontal structure concurred with the location of hot spots of fitted MI as well as with the location of bycaught common dolphin strandings, mainly occurring on the coast of the south Finistère region during the summer mortality season (http://seamap.env.duke.edu).

4.1.3. Other drivers of seasonal differences

The distribution of common dolphins in the Bay of Biscay differs between seasons (Laran et al. 2017). In winter, they are more numerous on the shelf, whereas in summer they are mainly distributed on the shelf break. This probably results in spatial differences in the local abundance of common dolphin between seasons, directly affecting bycatch risk. Seasonal differences in bycatch-induced mortality may further be linked to annual biological cycles of common dolphins and fish. The calving and mating season of short-beaked common dolphins of the northeast Atlantic is from April to September, with a likely peak of activity in July and August (Murphy et al. 2005, 2009). Feeding strategies and movement patterns of dolphins differ during those periods, resulting in a different response to oceanographic processes. This could also be true with respect to dolphins' preys, many of which present an annual biological cycle. As for the fisheries, they might likewise change their searching strategies, or their fishing gear, depending on the season and target species. The fishing effort and fishing targeted areas also likely differ between seasons (ICES 2020). A combination of those parameters might affect the difference between the 2 seasons regarding patterns of oceanographic variables effects on bycatch mortality.

Although the mechanisms were different between winter and summer mortality seasons, an influence of oceanographic processes and especially seasonal thermal front structures was highlighted for the 2 seasons of mortality. The association between marine predator and thermal fronts was shown and studied elsewhere (Doniol-Valcroze et al. 2007, Gannier & Praca 2007, Cox et al. 2018, Scales et al. 2018), and thermal fronts were identified as priority conservation areas for marine megafauna (Scales et al. 2014). If correlations are complex and not straightforward, this study still provides first hints of an association between short-beaked common dolphins and this type of mesoscale frontal structure in the Bay of Biscay, likely linked to bycatch mortality.

4.2. Between-month variations

For all 3 oceanographic covariates, in winter, interpretation is further complicated as their effects on the mortality index often switched sign from one month to the next. From a statistical point of view, there could be 2 reasons for this. First, because we conducted different models for each month, there is no dependence between consecutive months. This could be improved by putting additional model structure such as a first order random walk for example. However, this would also substantially increase the computational burden, multiplying the number of observations (3487 spatial cells 'observed' once per month and per year, so 334 752 observations for the complete dataset). Second, it is likely that the effect of

oceanographic processes on the mortality of dolphins due to bycatch is not linear or additive. Non-linear relationships with environmental covariates are routinely evidenced in marine species distribution modelling (Forney 2000, Stoner et al. 2001, Tew Kai & Marsac 2010) and fisheries (Maury et al. 2001, Walsh & Kleiber 2001, Zagaglia et al. 2004) or even bycatch studies (Žydelis et al. 2011, Di Tullio et al. 2015, Hahlbeck et al. 2017). Given the extra complexity of our response variable, it is quite conceivable that the influence of oceanographic features on short-beaked common dolphins bycatch is not linear. Combined with the fact that oceanographic processes might have different effects depending on their location and timing of appearance (that might vary from month to month), it could explain changes in signs of mean monthly coefficients of the oceanographic covariates. Again, relaxing the linear assumption would be possible with, for example, functional regression, but is beyond the scope of the present study.

There could also be ecological reasons for these between month variations. The winter oceanographic dynamics of the Bay of Biscay is characterized by high-frequency processes with rapid changes, sometimes within a month. Changes in the sign of OVs effects on the MI could be due to dynamic processes affecting common dolphins and fisheries interactions. The possibility that the effect of OVs could change from one month to the next motivated the use of random slopes. Taking thermal fronts as an example: these can aggregate preys of both common dolphins and predatory fish and do not necessarily increase bycatch risk. If fronts are quite wide and persistent, they could be wide enough so that they could attract fisheries on, say, their shore side and common dolphin on their seaside: spatial overlap between common dolphins and fisheries would be limited. However, if thermal fronts are very spatially localized, then spatial overlap between common dolphin and fisheries could be substantial, and bycatch risk would be higher. Yet, the frontal dynamics in the Bay of Biscay shows seasonal and interannual variability (Yelekçi et al. 2017). The width and intensity of thermal fronts can therefore vary from one month to the next (and for a given month, from one year to the next), which may also explain fickle statistical relationships.

4.3. The bycatch mortality of 2019: a predictable event?

Bycatch mortality in 2019 was the highest ever observed on the French Atlantic coast (Peltier et al. 2019), exceeding 2017 levels that were also unprecedented at that time. Still, crossvalidation results suggested it was statistically predictable as the observed monthly mortality tally from the dataset was within the confidence interval of the prediction (Fig. 7). Furthermore, results of the repetition scenarios showed how 2019's mortality was possibly due to circumstances already met in the past, either related to oceanographic conditions, or to other component included in models through the spatial process. The MI in 2019 was more accurately predicted when 2019 was considered as a repetition of 2013 and 2017 (Table 1, Fig. 7). For RS 2019 = 2017, the observed monthly mortality of 2019 was close to predicted values from oceanographic covariates (in 2019) and past relationships with OVs, both for winter and summer mortality seasons. As mentioned above, bycatch mortality in 2017 was also unprecedented at that time as an all-high record. 2017 indeed stands out as a singular year regarding the effect of all 3 covariates on bycatch risk (Fig. 5). This suggests maybe singular oceanographic phenomena in 2017 that were especially conductive of bycatch events, phenomena which recurred in 2019. A more surprising result was the remarkable good prediction made for winter months, when 2019 was considered as a repetition of 2013 (RS 2019 = 2013). Observed mortality in 2013 from the dataset was 156 individuals (as fresher stranded carcasses showing bycatch evidence or stranded during an intense mortality event, see Section 2), whereas it was 317 in 2017 and 413 in 2019, through January, February and March. However, the observed mortality in January 2013 was close to that of January 2017 (Fig. 3) and was the second highest value for this month in the study period. In addition, mean coefficient estimates of *eke* and *sst* were part of the highest from 2012 to 2018. In January, the mean coefficient estimate of *mean_sst_grad* in 2013 was close to the mean coefficient estimate in 2017. In January, the mean effect of the mean temperature gradient was also the same in 2013 and in 2017. Despite the lower levels of observed mortality in 2013, it seems that winter oceanographic conditions in 2013, 2017 and 2019 favored common dolphin and fishery interactions, with an intensifying trend over the years. Given the complexity of our results regarding oceanographic covariate effects on bycatch risk (with inter-annual and between-month variations), the additional value of repetition scenarios was to highlight whether similar associations occurred in different years.

Overall, these results showed that, from a statistical point of view, with few oceanographic covariates,

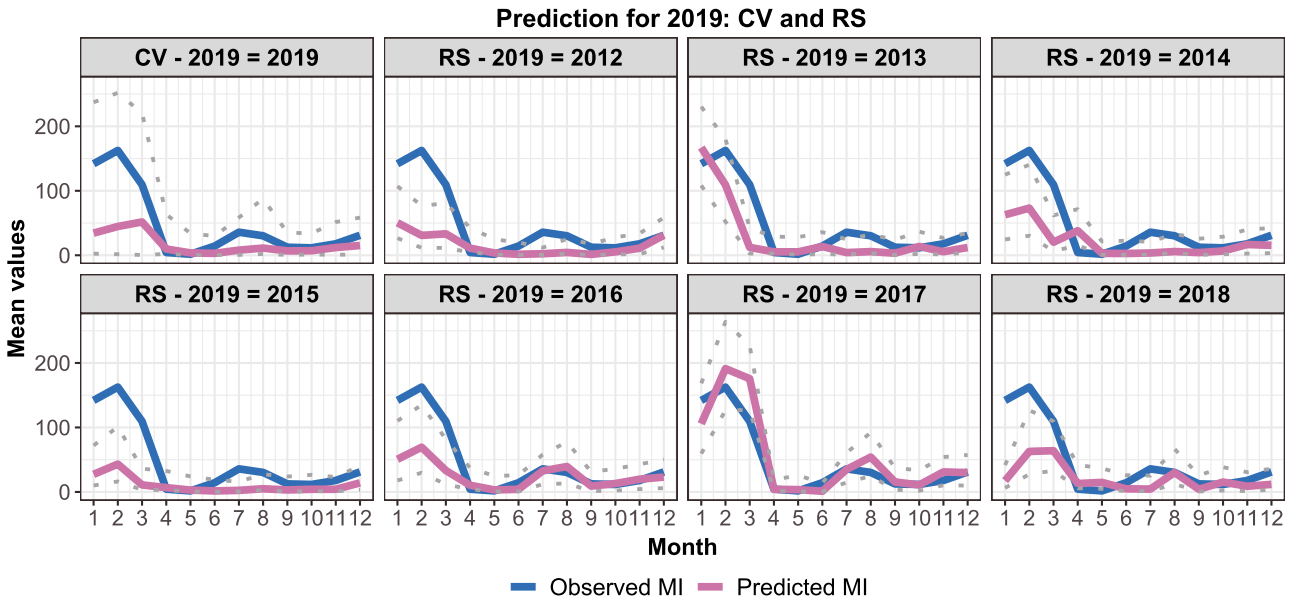

Fig. 7. Prediction for 2019. Monthly total mean mortality index from the dataset ('Observed MI') and from fitted values ('Predicted MI') for 2019 resulting from the 12 spatiotemporal models inferred with integrated nested Laplace approximations (INLA), with (1) a cross-validation (CV) procedure, i.e. the mortality index was predicted from previous years data and from values of oceanographic covariates for 2019 (2) repetition scenarios (RS), analogous to the latter except 2019 was considered as a repetition of a previous year of the study period. Grey dotted lines: 95%CI of fitted values

the unprecedented bycatch mortality of 2019 was at the very least unsurprising as the pattern observed in 2019 could be accurately predicted from 2012–2018 data. This highlights how gaining knowledge about environmental influences on interactions between short-beaked common dolphins and fisheries could have great conservation and management value (Scales et al. 2018). In this study, we adopted a modelling approach to determine whether bycatch mortality can be explained by oceanographic processes. However, with evidenced oceanographic influences on bycatch incidence, a similar analysis could be designed to forecast potential hotspots of mortality. The modelling approach would have to be different, as explanatory and predictive modelling are distinct and are associated with different 'modelling paths' (Shmueli 2010). For example, other sources of environmental data, available in a smaller timeframe, might have to be considered for near real-time prediction. Remote sensing could be an option, as it is already used in the support of fisheries activities (Santos 2000). The forecasting of high mortality zones might make it possible to define dynamic time–area closures for fisheries (Cosandey-Godin et al. 2015), which represent a promising tool to reduce bycatch pressure on the common dolphin population while limiting the economic impact (Dunn et al. 2011, Maxwell et al. 2015, Hazen et al. 2018). In this regard, further studies modelling the dynamic distribution of areas of co-occurrence of both short-beaked common dolphins and fisheries in the Bay of Biscay would be highly valuable for the conservation of this population.

4.4. Limitations and prospects for improvement

Several limitations can be imposed regarding the present work and results. First of all, strandings give only minimal estimations of bycatch-caused mortality. Some carcasses may never strand, and some others strand in advanced states of decomposition that do not allow their examination nor the identification of the cause of death of the animals. Moreover, due to the reverse drift modelling, the MI is associated with an uncertainty that is difficult to measure completely. Peltier et al. (2012) quantified the average distance between observed stranding locations of animals that were tagged when released from fishing boats and stranding locations predicted with MOTHY (27.1 ±

Table 1. Root mean squared error (RMSE) for cross-validation (CV) and repetition scenarios (RS)

	CV	RS						
	2019	2012	2013	2014	2015	2016	2017	2018
RMSE	48.4	51.2	32.8	43.6	54.2	45.0	30.1	48.1

24.5 km), which is accurate enough for practical purposes. Yet, there is no estimate of uncertainty associated with drift points as no information is available on where dolphins died. Developing the reverse modelling approach, on which the MI depends, was precisely motivated by infering high-probability at-sea mortality areas (Peltier & Ridoux 2015, Peltier et al. 2020).

The spatial scale for the present analysis (approximately 89 km^{-2}) was coarse compared to that of OVs. This coarse resolution required upscaling for OVs, which could have smoothed out too many high frequency processes such as fronts and eddies. It is thus possible that the relationship between the MI and OVs was weakened, impacting the results concerning oceanographic coefficients and explanatory power. The association between the MI and oceanographic variables is likely scale dependent as are associations between oceanographic covariates and marine top predators' distribution and foraging (Logerwell & Hargreaves 1996, Fauchald et al. 2000, Pinaud & Weimerskirch 2005, Pirotta et al. 2014). The link of interest here could be detectable at a specific spatial scale and not at another, and for high frequency processes the scale could be relatively small. Getting mortality data at a finer scale (and defining the spatial uncertainty associated with the reverse drift modelling) would then improve our understanding of the physical and ecological processes at stake.

Lastly, the models we developed for this study accounted for a low proportion of variance of the MI (25% at the highest, in February). This limits the range for interpretation, especially for months when this proportion was below 10%. This was expected: we aimed at quantifying links that are, at best, indirect between OVs and a marine top predator. Many trophic levels might be involved in the relationships of interest here, from phytoplankton to zooplankton and fish, each of these levels being influenced by several environmental and physiological factors. Moreover, the response variable we used is only a proxy of realized bycatch risk. Nonetheless, models performed well enough to reproduce annual patterns of total monthly MI from 2012 to 2018 (Appendix). Models performed better for the winter season with increased mortality and to a lesser extent for the summer mortality season, which were of particular interest regarding the seasonal pattern of bycatch. The CV results finally confirmed the acceptable performance of our models, suggesting an association between chosen oceanographic variables and bycatch-induced mortality of common dolphins in the Bay of Biscay.

This association should not be over-interpreted: relationships highlighted here are not straightforward, and they have been highlighted only for a few months, and not for all years. The limited explanatory power of the oceanographic covariates even for months when bycatch mortality was relatively high suggests that bycatch risk in the Bay of Biscay may be influenced by other non-environmental factors, e.g. characteristics of fisheries like the type of fishing gear used, the overall fishing effort or the timeline of the fishing operation (day or night). There were no significant changes in the pattern of the relationship between oceanographic processes and bycatch risk that could help explain the rise in bycatch observed from 2016 onward. This further suggests an influence of additional factors not considered in the present study. This rise of bycatch could be associated with a change in the distribution of common dolphins in the Bay of Biscay or a change in fishing practices. Bycatch risk is likely affected by a mix of different factors, oceanographic processes being one among others.

5. CONCLUSIONS

This study demonstrated the relevance of stranding data and modelled OVs from coastal operational oceanography to better understand this intense bycatch phenomenon which causes a serious threat to the short-beaked common dolphin population of the northeast Atlantic (Peltier et al. 2016, Murphy et al. 2019). The need to explicitly integrate spatial and temporal dimensions for such complex interactions was justified: our results effectively highlighted the spatiotemporal influences of structuring oceanographic processes on the risk of common dolphin bycatch in the Bay of Biscay. However, the underlying mechanisms remain unclear, and the relationship between environmental characteristics and dolphin bycatch must not be overinterpreted, as our model only indirectly links OVs with dolphin bycatch. Because of the dynamic aspects of both structuring oceanographic processes and dolphin and fishery distributions, further research focusing on smaller time scales is needed. For instance, extreme stranding events are observed on a weekly timeframe (Peltier et al. 2020), suggesting short periods of intense interactions between dolphins and fisheries, so a similar analysis on a weekly timeframe and focusing on these events might be more informative. Furthermore, we showed that the pattern of seasonal bycatch events can be directly inferred from past data on strandings and oceanographic conditions. This

highlights the value of establishing functional relationships to eventually identify adapted and acceptable management measures to ensure both the long-term conservation of the population of short-beaked common dolphins of the Bay of Biscay and fisheries activities.

Acknowledgements. We warmly thank all members of the French and UK stranding networks for their continuous effort in collecting stranding data. We thank Marie-Pierre Etienne and Etienne Rivot for their insightful comments on our work. We also thank the community participating in the development of INLA, and especially Havard Rue for his devotion towards helping INLA users. Finally, we thank the reviewers for their insightful comments which helped to significantly improve the quality of the manuscript. The Observatoire PELAGIS is funded by the ministry in charge of the environment, and by Communauté d'Agglomération de la Ville de La Rochelle, with support from Région Poitou-Charentes and the European Union. EOVs were computed by the Shom and partially funded by the ministry in charge of the environment under the Marine Strategy Framework Directive (MSFD) monitoring program.

LITERATURE CITED

Bailey H, Thompson P (2010) Effect of oceanographic features on fine-scale foraging movements of bottlenose dolphins. Mar Ecol Prog Ser 418:223–233

Bakun A (1996) Patterns in the ocean: ocean processes and marine population dynamics. California Sea Grant, La Jolla, CA

Bakun A (2006) Fronts and eddies as key structures in the habitat of marine fish larvae: opportunity, adaptive response and competitive advantage. Sci Mar 70(S2):105–122

Barlow DR, Bernard KS, Escobar-Flores P, Palacios DM, Torres LG (2020) Links in the trophic chain: modeling functional relationships between *in situ* oceanography, krill, and blue whale distribution under different oceanographic regimes. Mar Ecol Prog Ser 642:207–225

Becker EA, Forney KA, Ferguson MC, Foley DG, Smith RC, Barlow J, Redfern JV (2010) Comparing California current cetacean–habitat models developed using *in situ* and remotely sensed sea surface temperature data. Mar Ecol Prog Ser 413:163–183

Besag J, Kooperberg C (1995) On conditional and intrinsic autoregressions. Biometrika 82:733–746

Besag J, York J, Mollié A (1991) A Bayesian image restoration with two applications in spatial statistics. Ann Inst Stat Math 43:1–59

Best BD, Halpin PN, Read AJ, Fujioka E and others (2012) Online cetacean habitat modeling system for the US East Coast and Gulf of Mexico. Endang Species Res 18:1–15

Blangiardo M, Cameletti M, Baio G, Rue H (2013) Spatial and spatio-temporal models with R-INLA. Spat Spatiotemporal Epidemiol 4:33–49

Bleck R (2002) An oceanic general circulation model framed in hybrid isopycnic-Cartesian coordinates. Ocean Model 4:55–88

Brownell RL Jr, Reeves RR, Read AJ, Smith BD and others (2019) Bycatch in gillnet fisheries threatens Critically Endangered small cetaceans and other aquatic megafauna. Endang Species Res 40:285–296

Castro J, Couto A, Borges FO, Cid A, Laborde MI, Pearson HC, Rosa R (2020) Oceanographic determinants of the abundance of common dolphins (*Delphinus delphis*) in the south of Portugal. Oceans 1:165–173

Cosandey-Godin A, Krainski ET, Worm B, Flemming JM (2015) Applying Bayesian spatiotemporal models to fisheries bycatch in the Canadian Arctic. Can J Fish Aquat Sci 72:186–197

Cox SL, Embling CB, Hosegood PJ, Votier SC, Ingram SN (2018) Oceanographic drivers of marine mammal and seabird habitat-use across shelf-seas: a guide to key features and recommendations for future research and conservation management. Estuar Coast Shelf Sci 212: 294–310

Croll DA, Tershy BR, Hewitt RP, Demer DA and others (1998) An integrated approch to the foraging ecology of marine birds and mammals. Deep Sea Res II 45:1353–1371

D'Agrosa C, Lennert-Cody CE, Vidal O (2000) Vaquita bycatch in Mexico's artisanal gillnet fisheries: driving a small population to extinction. Conserv Biol 14:1110–1119

Daniel P, Jan G, Cabioc'h F, Landau Y, Loiseau E (2002) Drift modeling of cargo containers. Spill Sci Technol Bull 7: 279–288

Dars C, Dabin W, Demaret F, Meheust E and others (2019) Les échouages de mammifères marins sur le littoral français en 2019. Rapport scientifique de l'Observatoire Pelagis, La Rochelle Université et CNRS

Di Tullio JC, Fruet PF, Secchi ER (2015) Identifying critical areas to reduce bycatch of coastal common bottlenose dolphins *Tursiops truncatus* in artisanal fisheries of the subtropical western South Atlantic. Endang Species Res 29:35–50

Díaz López B, Methion S, Giralt Paradell O (2019) Living on the edge: overlap between a marine predator's habitat use and fisheries in the northeast Atlantic waters (NW Spain). Prog Oceanogr 175:115–123

Doniol-Valcroze T, Berteaux D, Larouche P, Sears R (2007) Influence of thermal fronts on habitat selection by four rorqual whale species in the Gulf of St. Lawrence. Mar Ecol Prog Ser 335:207–216

Dunn DC, Boustany AM, Halpin PN (2011) Spatio-temporal management of fisheries to reduce by-catch and increase fishing selectivity. Fish Fish 12:110–119

Fauchald P, Erikstad KE, Skarsfjord H (2000) Scale-dependent predator–prey interactions: the hierarchical spatial distribution of seabirds and prey. Ecology 81:773–783

Fioravanti G, Martino S, Cameletti M, Cattani G (2021) Spatio-temporal modelling of PM10 daily concentrations in Italy using the SPDE approach. Atmos Environ 248:118192

Forney KA (2000) Environmental models of cetacean abundance: reducing uncertainty in population trends. Conserv Biol 14:1271–1286

Gabry J, Simpson D, Vehtari A, Betancourt M, Gelman A (2019) Visualization in Bayesian workflow. J R Stat Soc Ser A Stat Soc 182:389–402

Gannier A, Praca E (2007) SST fronts and the summer sperm whale distribution in the northwest Mediterranean Sea. J Mar Biol Assoc UK 87:187–193

García-Barón I, Santos MB, Saavedra C, Astarloa A, Valeiras J, García Barcelona S, Louzao M (2020) Essential ocean variables and high value biodiversity areas: targets for the conservation of marine megafauna. Ecol Indic 117:106504

Gardner B, Sullivan PJ, Epperly S, Morreale SJ (2008) Hierarchical modeling of bycatch rates of sea turtles in the western North Atlantic. Endang Species Res 5:279–289

Gelman A, Hwang J, Vehtari A (2014) Understanding predictive information criteria for Bayesian models. Stat Comput 24:997–1016

Hahlbeck N, Scales KL, Dewar H, Maxwell SM, Bograd SJ, Hazen EL (2017) Oceanographic determinants of ocean sunfish (*Mola mola*) and bluefin tuna (*Thunnus orientalis*) bycatch patterns in the California large mesh drift gillnet fishery. Fish Res 191:154–163

Hazen EL, Scales KL, Maxwell SM, Briscoe DK and others (2018) A dynamic ocean management tool to reduce bycatch and support sustainable fisheries. Sci Adv 4:eaar3001

Hughes KM, Dransfeld L, Johnson MP (2014) Changes in the spatial distribution of spawning activity by north-east Atlantic mackerel in warming seas: 1977–2010. Mar Biol 161:2563–2576

Huret M, Bourriau P, Doray M, Gohin F, Petitgas P (2018) Survey timing vs. ecosystem scheduling: degree-days to underpin observed interannual variability in marine ecosystems. Prog Oceanogr 166:30–40

Hyrenbach DK, Forney KA, Dayton PK (2000) Viewpoint: marine protected areas and ocean basin management. Aquat Conserv 10:437–458

ICES (2020) Workshop on fisheries emergency measures to minimize bycatch of short-beaked common dolphins in the Bay of Biscay and harbour porpoise in the Baltic Sea (WKEMBYC). ICES Sci Rep 2:354

Ijsseldijk LL, ten Doeschate MT, Brownlow A, Davison NJ and others (2020) Spatiotemporal mortality and demographic trends in a small cetacean: strandings to inform conservation management. Biol Conserv 249:108733

Jaramillo-Legorreta A, Rojas-Bracho L, Brownell RL Jr, Read AJ, Reeves RR, Ralls K, Taylor BL (2007) Saving the vaquita: immediate action, not more data. Conserv Biol 21:1653–1655

Jaramillo-Legorreta AM, Cardenas-Hinojosa G, Nieto-Garcia E, Rojas-Bracho L and others (2019) Decline towards extinction of Mexico's vaquita porpoise (*Phocoena sinus*). R Soc Open Sci 6:190598

Johnson PC (2014) Extension of Nakagawa & Schielzeth's R2GLMM to random slopes models. Methods Ecol Evol 5:944–946

Kuiken T (1994) Diagnosis of bycatch in cetaceans. Proceedings of the Second ECS Workshop on Cetacean Pathology. European Cetacean Society, Montpellier

Lahaye S, Gouillon F, Baraille R, Pichon A, Pineau-Guillou L, Morel Y (2011) A numerical scheme for modeling tidal wetting and drying. J Geophys Res Oceans 116:1–20

Lambert C, Virgili A, Pettex E, Delavenne J, Toison V, Blanck A, Ridoux V (2017) Habitat modelling predictions highlight seasonal relevance of marine protected areas for marine megafauna. Deep Sea Res II 141:262–274

Lanz E, López-Martínez J, Nevárez-Martínez M, Dworak JA (2009) Small pelagic fish catches in the Gulf of California associated with sea surface temperature and chlorophyll. CCOFI Rep 50:134–146

Laran S, Authier M, Blanck A, Doremus G and others (2017) Seasonal distribution and abundance of cetaceans within French waters — Part II. The Bay of Biscay and the English Channel. Deep Sea Res II 141:31–40

Legendre P, Dale MR, Fortin MJ, Gurevitch J, Hohn M, Myers D (2002) The consequences of spatial structure for the design and analysis of ecological field surveys. Ecography 25:601–615

Levin SA (1992) The problem of pattern and scale in ecology. Ecology 73:1943–1967

Lewison RL, Crowder LB, Read AJ, Freeman SA (2004) Understanding impacts of fisheries bycatch on marine megafauna. Trends Ecol Evol 19:598–604

Logerwell EA, Hargreaves NB (1996) The distribution of sea birds relative to their fish prey off Vancouver Island: opposing results at large and small spatial scales. Fish Oceanogr 5:163–175

Mannocci L, Dabin W, Augeraud-Véron E, Dupuy JF, Barbraud C, Ridoux V (2012) Assessing the impact of bycatch on dolphin populations: the case of the common dolphin in the Eastern North Atlantic. PLOS ONE 7: e32615

Martínez-Minaya J, Cameletti M, Conesa D, Pennino MG (2018) Species distribution modeling: a statistical review with focus in spatio–temporal issues. Stochastic Environ Res Risk Assess 32:3227–3244

Maury O, Gascuel D, Marsac F, Fonteneau A, Rosa ALD (2001) Hierarchical interpretation of nonlinear relationships linking yellowfin tuna (*Thunnus albacares*) distribution to the environment in the Atlantic Ocean. Can J Fish Aquat Sci 58:458–469

Maxwell SM, Hazen EL, Lewison RL, Dunn DC and others (2015) Dynamic ocean management: defining and conceptualizing real-time management of the ocean. Mar Policy 58:42–50

Mellin C, Russell BD, Connell SD, Brook BW, Fordham DA (2012) Geographic range determinants of two commercially important marine molluscs. Divers Distrib 18: 133–146

Miller PI, Scales KL, Ingram SN, Southall EJ, Sims DW (2015) Basking sharks and oceanographic fronts: quantifying associations in the north-east Atlantic. Funct Ecol 29:1099–1109

Moore MJ, Mitchell GH, Rowles TK, Early G (2020) Dead cetacean? Beach, bloat, float, sink. Front Mar Sci 7:333

Moraga P (2019) Geospatial health data: modeling and visualization with R-INLA and Shiny. CRC Press, Boca Raton, FL

Morel Y, Baraille R, Pichon A (2008) Time splitting and linear stability of the slow part of the barotropic component. Ocean Model 23:73–81

Murphy S, Collet A, Rogan E (2005) Mating strategy in the male common dolphin (*Delphinus delphis*): what gonadal analysis tells us. J Mammal 86:1247–1258

Murphy S, Winship A, Dabin W, Jepson PD and others (2009) Importance of biological parameters in assessing the status of *Delphinus delphis*. Mar Ecol Prog Ser 388: 273–291

Murphy S, Evans PG, Pinn E, Pierce GJ (2019) Conservation management of common dolphins: lessons learned from the north-east Atlantic. Aquat Conserv 131:137–166

Murray KT, Orphanides CD (2013) Estimating the risk of loggerhead turtle *Caretta caretta* bycatch in the US mid-Atlantic using fishery-independent and -dependent data. Mar Ecol Prog Ser 477:259–270

Nel DC, Lutjeharms JRE, Pakhomov EA, Ansorge IJ, Ryan PG, Klages NTW (2001) Exploitation of mesoscale oceanographic features by grey-headed albatross *Thalassarche chrysostoma* in the southern Indian Ocean. Mar Ecol Prog Ser 217:15–26

Norris KS, McFarland WN (1958) A new harbor porpoise of the genus *Phocoena* from the Gulf of California. J Mammal 39:22

Pebesma E (2018) Simple features for R: standardized support for spatial vector data. R J 10:439–446

Peltier H, Ridoux V (2015) Marine megavertebrates adrift: a framework for the interpretation of stranding data in perspective of the European Marine Strategy Framework Directive and other regional agreements. Environ Sci Policy 54:240–247

Peltier H, Dabin W, Daniel P, Van Canneyt O, Dorémus G, Huon M, Ridoux V (2012) The significance of stranding data as indicators of cetacean populations at sea: modelling the drift of cetacean carcasses. Ecol Indic 18:278–290

Peltier H, Baagøe HJ, Camphuysen KC, Czeck R and others (2013) The stranding anomaly as population indicator: the case of harbour porpoise *Phocoena phocoena* in north-western Europe. PLOS ONE 8:e62180

Peltier H, Jepson PD, Dabin W, Deaville R, Daniel P, Van Canneyt O, Ridoux V (2014) The contribution of stranding data to monitoring and conservation strategies for cetaceans: developing spatially explicit mortality indicators for common dolphins (*Delphinus delphis*) in the eastern North-Atlantic. Ecol Indic 39:203–214

Peltier H, Authier M, Deaville R, Dabin W and others (2016) Small cetacean bycatch as estimated from stranding schemes: the common dolphin case in the northeast Atlantic. Environ Sci Policy 63:7–18

Peltier H, Authier M, Caurant F, Dabin W, Dars C and others (2019) Etat des connaissances sur les captures accidentelles de dauphins communs dans le golfe de Gascogne – Synthèse 2019. Rapport scientifique dans le cadre de la convention avec le MTES. Technical report, Observatoire PELAGIS — UMS 3462, La Rochelle Université/CNRS

Peltier H, Authier M, Dabin W, Dars C and others (2020) Can modelling the drift of bycaught dolphin stranded carcasses help identify involved fisheries? An exploratory study. Glob Ecol Conserv 21:e00843

Peltier H, Authier M, Caurant F, Dabin W and others (2021) In the wrong place at the wrong time: identifying spatiotemporal co-occurrence of bycaught common dolphins and fisheries in the Bay of Biscay (NE Atlantic) from 2010 to 2019. Front Mar Sci 8:617342

Petitgas P, Doray M, Huret M, Masse J, Woillez M (2014) Modelling the variability in fish spatial distributions over time with empirical orthogonal functions: anchovy in the Bay of Biscay. ICES J Mar Sci 71:2379–2389

Pichon A, Correard S (2006) Internal tides modelling in the Bay of Biscay. Comparisons with observations. Sci Mar 70(S1):65–88

Pichon A, Morel Y, Baraille R, Quaresma LS (2013) Internal tide interactions in the Bay of Biscay: observations and modelling. J Mar Syst 109–110(Suppl):S26–S44

Pinaud D, Weimerskirch H (2005) Scale-dependent habitat use in a long-ranging central place predator. J Anim Ecol 74:852–863

Pirotta E, Thompson PM, Miller PI, Brookes KL and others (2014) Scale-dependent foraging ecology of a marine top predator modelled using passive acoustic data. Funct Ecol 28:206–217

Planque B, Bellier E, Lazure P (2007) Modelling potential spawning habitat of sardine (*Sardina pilchardus*) and anchovy (*Engraulis encrasicolus*) in the Bay of Biscay. Fish Oceanogr 16:16–30

Politikos DV, Huret M, Petitgas P (2015) A coupled movement and bioenergetics model to explore the spawning migration of anchovy in the Bay of Biscay. Ecol Model 313:212–222

R Core Team (2020) R: a language and environment for statistical computing. R Foundation for Statistical Computing, Vienna

Reeves RR, Berggren P, Crespo EA, Gales N and others (2005) Global priorities for reduction of cetacean bycatch. Technical report. World Wildlife Fund

Rue H, Martino S, Chopin N (2009) Approximate Bayesian inference for latent Gaussian models by using integrated nested Laplace approximations. J R Stat Soc Series B Stat Methodol 71:319–392

Santos AMP (2000) Fisheries oceanography using satellite and airborne remote sensing methods: a review. Fish Res 49:1–20

Scales KL, Miller PI, Hawkes LA, Ingram SN, Sims DW, Votier SC (2014) On the front line: frontal zones as priority at-sea conservation areas for mobile marine vertebrates. J Appl Ecol 51:1575–1583

Scales KL, Hazen EL, Jacox MG, Castruccio F, Maxwell SM, Lewison RL, Bograd SJ (2018) Fisheries bycatch risk to marine megafauna is intensified in Lagrangian coherent structures. Proc Natl Acad Sci USA 115:7362–7367

Shmueli G (2010) To explain or to predict? Stat Sci 25:289–310

Snyder S, Franks PJS, Talley LD, Xu Y, Kohin S (2017) Crossing the line: tunas actively exploit submesoscale fronts to enhance foraging success. Limnol Oceanogr Lett 2:187–194

Spitz J, Chouvelon T, Cardinaud M, Kostecki C, Lorance P (2013) Prey preferences of adult sea bass *Dicentrarchus labrax* in the northeastern Atlantic: implications for bycatch of common dolphin *Delphinus delphis*. ICES J Mar Sci 70:452–461

Stephenson F, Goetz K, Sharp BR, Mouton TL and others (2020) Modelling the spatial distribution of cetaceans in New Zealand waters. Divers Distrib 26:495–516

Stoner AW, Manderson JP, Pessutti JP (2001) Spatially explicit analysis of estuarine habitat for juvenile winter flounder: combining generalized additive models and geographic information systems. Mar Ecol Prog Ser 213:253–271

Tew Kai E, Marsac F (2010) Influence of mesoscale eddies on spatial structuring of top predators' communities in the Mozambique Channel. Prog Oceanogr 86:214–223

Tew-Kai E, Quilfen V, Cachera M, Boutet M (2020) Dynamic coastal-shelf seascapes to support marine policies using operational coastal oceanography: the French example. J Mar Sci Eng 8:585

Tobler WR (1970) A computer movie simulating urban growth in the Detroit region. Econ Geogr 46:234

Turvey ST, Pitman RL, Taylor BL, Barlow J and others (2007) First human-caused extinction of a cetacean species? Biol Lett 3:537–540

Valcu M, Kempenaers B (2010) Spatial autocorrelation: an overlooked concept in behavioral ecology. Behav Ecol 21:902–905

Walsh WA, Kleiber P (2001) Generalized additive model and regression tree analyses of blue shark (*Prionace glauca*) catch rates by the Hawaii-based commercial longline fishery. Fish Res 53:115–131

Watanabe S (2010) Asymptotic equivalence of Bayes cross validation and widely applicable information criterion in singular learning theory. J Mach Learn Res 11:3571–3594

Weltz K, Kock AA, Winker H, Attwood C, Sikweyiya M (2013) The influence of environmental variables on the

presence of white sharks, *Carcharodon carcharias* at two popular Cape Town bathing beaches: a generalized additive mixed model. PLOS ONE 8:e68554

Yelekçi Ö (2017) Submesoscale dynamics in the Bay of Biscay continental. PhD, Université Pierre et Marie Curie – Paris VI

Yelekçi Ö, Charria G, Capet X, Reverdin G, Sudre J, Yahia H (2017) Spatial and seasonal distributions of frontal activity over the French continental shelf in the Bay of Biscay. Cont Shelf Res 144:65–79

Zagaglia CR, Lorenzzetti JA, Stech JL (2004) Remote sensing data and longline catches of yellowfin tuna (*Thunnus albacares*) in the equatorial Atlantic. Remote Sens Environ 93:267–281

Zuur A, Ieno EN, Smith GM (2007) Analyzing ecological data, Chaps 6 & 7. Springer, New York, NY

Žydelis R, Lewison RL, Shaffer SA, Moore JE and others (2011) Dynamic habitat models: using telemetry data to project fisheries bycatch. Proc R Soci B Biol Sci 278: 3191–3200

Appendix.

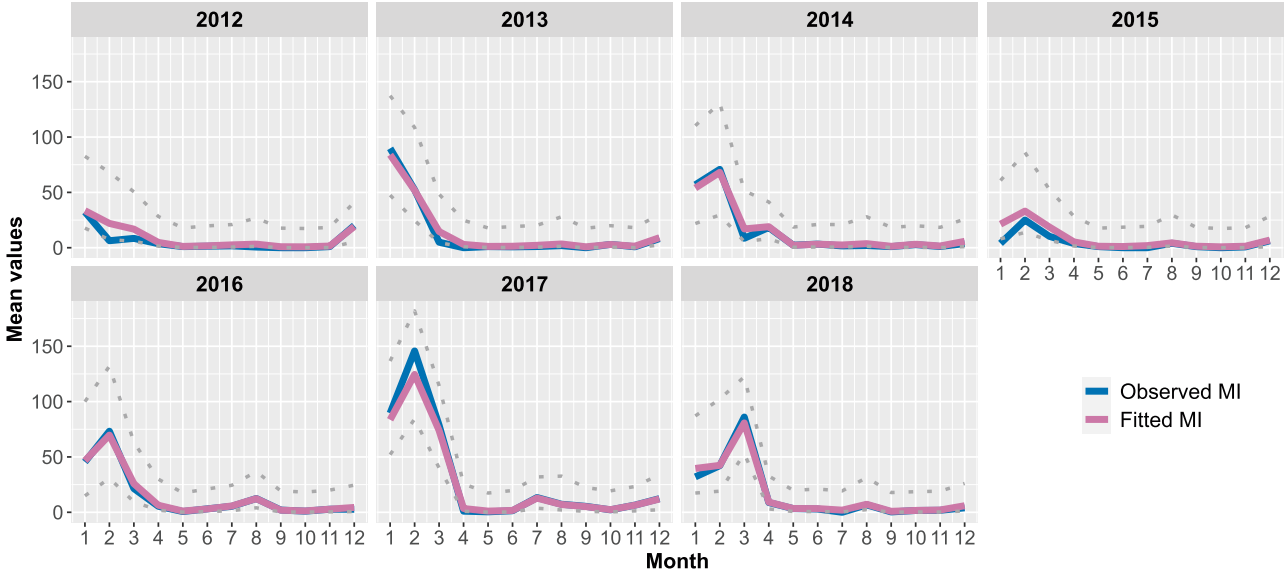

Fig. A1. Temporal series of the monthly total mean mortality index from the dataset ('observed', in blue) and from fitted values ('fitted', in purple) resulting from the 12 spatiotemporal models inferred with integrated nested Laplace approximations (INLA), from 2012 to 2018. Grey dotted lines: sum of the 0.025 (lower bound) and 0.975 (upper bound) quantiles of fitted values

Editorial responsibility: Elliott Hazen, Pacific Grove, California, USA
Reviewed by: I. Paradinas and 2 anonymous referees

Submitted: March 15, 2021
Accepted: September 7, 2021
Proofs received from author(s): November 19, 2021